Morphology of Polythiophene and Polyphenyl Films Produced via Surface Polymerization by Ion-Assisted Deposition†

Sanja Tepavcevic, Adam M. Zachary, Amanda T. Wroble, Yongsoo Choi, and Luke Hanley*

Department of Chemistry (m/c 111), University of Illinois at Chicago, Chicago, Illinois 60607-7061

Received: July 30, 2005; In Final Form: August 31, 2005

Conducting polymer films are grown by either mass-selected or non-mass-selected, hyperthermal thiophene ions coincident on a surface with a thermal beam of organic monomers of either α-terthiophene (3T) or *p*-terphenyl (3P) neutrals. Previous experiments verified polymerization of both 3T and 3P by 200 eV $C_4H_4S^+$ during surface polymerization by ion-assisted deposition (SPIAD). A wide variety of structures are observed by scanning electron microscopy to form in the SPIAD polythiophene and polyphenyl films. These structures include microscale islands, lamellar structures, fractal-like growth patterns, and nanoscale crystallites. Some of the deposited films diffract X-rays while others show electron micrographs of crystallites. The variation of these patterns with deposition conditions clearly indicate that ion-induced polymerization mediates film morphology through control of ion energy and ion/neutral ratio. Furthermore, these ion-assisted events mediate important thermal processes such as sublimation.

I. Introduction

Control of film morphology is widely recognized as one of the limiting factors in the development of conjugated polymers for photonic and electronic applications such as organic thin film transistors, light-emitting diodes, photovoltaics, and sensors. Electronic properties of conjugated polymers such as charge mobility and injection depend strongly on molecular orientation and packing.[1−3] The inability to control film structure and morphology can lead to reduced efficiency in energy and charge transport processes.

Polythiophene, polyphenyl, and their substituted derivatives have been the subject of extensive research as a result of their useful chemical and electronic properties.[1,4] Semiconductive oligomers are attractive alternatives to conjugated polymers because they offer the advantage of presenting a well-defined chemical structure and easier processing than many polymers. Applications of conducting polymer layers are often limited not by the intrinsic charge carrier mobility in the material but rather by that of its film. New film growth methods are required that improve film electronic properties and are compatible with established manufacturing techniques.

Various routes can be followed for control of the structural organization of molecular and polymeric films. One can use a physical approach, involving either the modification of the experimental conditions during or after film deposition, or a chemical approach, by tailoring the molecular structure to influence the properties of self-assembled films.[5−8] High substrate temperature during thermal evaporative growth is effective for controlling the extent of grain boundaries and structural ordering in the aggregates but is less effective for the control of surface roughness. Furthermore, the gain in order is accompanied by a loss of compactness, which can lead to electrical leakages and short circuits in devices. Hyperthermal supersonic beam deposition of quaterthiophene (4T) onto room-temperature substrates produced films similar to those obtained by thermal evaporation onto substrates at temperatures above 300 K.[9−12]

Strategies utilizing polyatomic ion deposition display great promise for creation of new types of organic thin films including conducting polymers since these strategies allow control of film properties by selection of the ion structure, kinetic energy, or fluence.[13] Examples of this strategy include hyperthermal polyatomic ion-assisted deposition of conducting polymer thin films.[14,15] Film surface morphology and thickness of films from deposited hyperthermal polyatomic ions can also be controlled by their kinetic energy and fluence.[16,17]

Previous work has described surface polymerization by ion-assisted deposition (SPIAD)[18] in which a neutral beam of evaporated oligomers is polymerized on a surface by a separate beam of hyperthermal polyatomic ions to form a conducting polymer film. Polythiophene and polyphenyl SPIAD films have been produced by both mass-selected and non-mass-selected thiophene ion beams deposited with coincident α-terthiophene (3T) and *p*-terphenyl (3P) neutrals.[18−21] It was demonstrated that selection of ion structure, energy, and ion/neutral ratio can tune the polymerization and other ion-induced events that mediate thermal film growth through sputtering, bond breakage, energetic mixing, and other processes.[19] Control of nanoscale morphology in SPIAD is expected since hyperthermal polyatomic ions only interact with the top few nanometers of the surface upon initial impact and ion-induced processes will mediate deposition, sublimation, and diffusion which also affect morphology. Computer simulations and SPIAD experiments confirm that incident hyperthermal thiophene ions will produce fragments upon surface impact that react with 3T and initiate polymerization.[22] Excessive ion kinetic energy or fluence will enhance fragmentation, desorption, and sputtering which in turn will modulate film morphology. Control of film morphology is expected to lead to changes in film optical properties, but morphology and optical properties have not yet been directly correlated in SPIAD films. However, photoemission studies have shown that SPIAD conducting polymer films display new

† Part of the special issue "William Hase Festschrift".

* To whom correspondence should be addressed. E-mail: LHanley@uic.edu.

10.1021/jp054231+ CCC: $33.50
Published on Web 10/05/2005

valence band features resulting from a reduction in both their band gap and barrier to hole injection.[23] Furthermore, UV−vis absorption and photoluminescence spectra of SPIAD films produced by non-mass-selected ions can be controlled by both ion energy and ion/neutral ratio.[20] Scanning electron microscopy and X-ray diffraction are used here to demonstrate that ion kinetic energy and ion/neutral ratio in SPIAD control the morphology of polythiophene and polyphenyl films produced from mass-selected thiophene ions and either 3T or 3P, respectively. The morphology and crystallinity of SPIAD polythiophene films produced by mass-selected and non-mass-selected ions are also compared.

II. Experimental Section

A. Mass-Selected Deposition. SPIAD is performed by combining deposition of thiophene ions with simultaneous dosing of 3T or 3P. The vacuum apparatus for SPIAD film preparation and analysis is only briefly described here.[19,24] The apparatus consists of a differentially pumped ion source with an organic evaporator located in a preparation chamber, a separate analysis chamber, and a sample transfer stage to connect the two chambers. A constant ion current of 30 nA (ion fluence of 4×10^{15} ions/cm^2) and two ion energies, 100 and 200 eV, are used for film deposition. A constant 3T flux of 6×10^{17} neutrals/cm^2 corresponding to a 1/150 ion/neutral ratio is used for SPIAD polythiophene film deposition, and constant 3P flux of 4×10^{17} neutrals/cm^2 corresponding to a 1/100 ion/neutral ratio for SPIAD polyphenyl film deposition.

B. Non-mass-Selected Deposition. The experimental conditions and apparatus that include the ion source, mass flow controller, and energy analyzer/quadruple mass spectrometer were described previously.[17,20] A commercial Kaufman ion source (Veeco-CS 3 cm Ion Source) using 30 eV electron impact energy generates intact thiophene ions and fragments thereof. SPIAD polythiophene films are formed from non-mass-selected ion beams with 100 eV ion energy, thiophene ion fluence of 4×10^{16} ions/cm^2, and 3T neutral flux of 4×10^{18} neutrals/cm^2.

Silicon wafers are used as substrates, after etching with 5% HF to produce the hydrogen-terminated surface H−Si(100) with a minimum of oxide. The HF-etched silicon surfaces prior to deposition display an elemental content of 10% carbon, 4% oxygen, and 86% silicon.[19]

C. Scanning Electron Microscopy (SEM). The scanning electron microscope (Hitachi S-3000N) is used in high-vacuum mode for films from mass-selected deposition. Variable-pressure mode is used for films from non-mass-selected deposition due to charging that results from their much greater thicknesses. Accelerating voltages of 3−5 keV are used, leading to effective magnifications of 1000−3000×. A 50 nm resolution is obtained with secondary electron ionization used for mass-selected SPIAD films, and 100 nm resolution is obtained with backscattered electrons used for non-mass-selected SPIAD films. A higher magnification SEM **(**JEOL JSM-6320F) with cold field emission source is used to further examine closely spaced features at an acceleration voltage of 4 keV and magnification of 25 000× at a 9 mm working distance.

D. X-ray Diffraction (XRD). The XRD analysis is carried out on a standard powder diffractometer (Siemens D-5000) using the Bragg−Brentano method ($\theta-2\theta$) in symmetric reflection mode with Cu Kα radiation selected by a graphite monochromator.

E. Morphological Analysis of X-ray Photoelectron Spectroscopy (XPS) Data. XPS analysis of the SPIAD polythiophene and polyphenyl was previously reported.[19] Quantitative Analysis of Surfaces by Electron Spectroscopy software (QUASES, Tougaard APS, Odense, Denmark) is used here to estimate the SPIAD film morphology within the XPS sampling depth.[25,26] QUASES relies on the observation that the inelastically scattered energy loss structure of X-ray photoelectron spectra carries information on the depth of origin of the detected electrons. The background of the entire survey scan is used for QUASES analysis, but most of the inelastically scattered background derives from the carbon and sulfur core level electrons from the films as the silicon substrate signal is relatively low. The attenuation length used in QUASES computations are approximated by an inelastic mean free path value of 30 Å, although values of 25 Å give similar results. The data are fit by a passive island model using polymer cross sections developed by Tougaard,[25,26] with an *x*-scale value of 1.09.

III. Results

A. 3T SPIAD Films from Mass-Selected Ions. A polythiophene film is prepared by SPIAD using the previously determined optimal conditions of 1/150 fluence ratio of 200 eV mass-selected thiophene ions ($C_4H_4S^+$) to evaporated 3T neutrals.[19] Previous experimental work determined many of the chemical and electronic properties of these polythiophene films.[19,23] X-ray photoelectron spectroscopy (XPS) showed much higher film formation efficiency for SPIAD polythiophene than for direct thiophene ion deposition. Various polymerization products were observed by mass spectrometric analysis including adducts of 3T with thiophene ions or fragments thereof including $[3T]T^+$ and multiple 3T adducts including $[3T]_2^+$. X-ray photoelectron C_{1s} binding energies and peak widths for the polythiophene films were also consistent with such a multicomponent system. SPIAD polythiophene films showed a reduction in band gap and barrier to hole injection compared to evaporated 3T films, as determined by ultraviolet photoelectron spectroscopy and near-edge X-ray absorption fine structure (NEXAFS).[23] Finally, these polythiophene films were found to be stable in a vacuum over a period during which evaporated 3T films completely sublime. All these results are consistent with polymerization of the 3T neutrals to form a polythiophene film composed of a distribution of higher molecular weight oligomers with an extended electron conjugation length.

Figure 1 shows the scanning electron microscopy (SEM) images of 3T evaporated and SPIAD films prepared at 1/150 ion/neutral ratio and 200 eV ion energy. The 10 μm scale SEM image of the 3T evaporated film in Figure 1a shows compact grains of various orientation, shapes, and dimensions of 1−5 μm on a side. The similarly scaled SEM image of the 3T SPIAD film in Figure 1b appears distinctly different, with elongated lamellar structures with feature sizes on the order 4 μm long by 0.3 μm wide. Furthermore, these lamellar features are interconnected, creating a network over the film surface. Similar features to those of the SPIAD film (Figure 1b) were observed previously for evaporation of sexithiophene (6T) onto high-temperature substrates.[6] The 50 μm image of the 3T SPIAD film in Figure 1c displays large rounded features, within one of which the Figure 1b image is recorded. These islands are mostly round with some slightly oval, and they vary in size from 10 to 90 μm in diameter. Lamellar features form only within the islands and the islands display well-defined edges.

The regions outside the islands in Figure 1c are featureless. These featureless regions are not bare silicon wafer surface, which also appears completely smooth on this size scale.[17] It is proposed that these featureless regions are a sulfur-containing

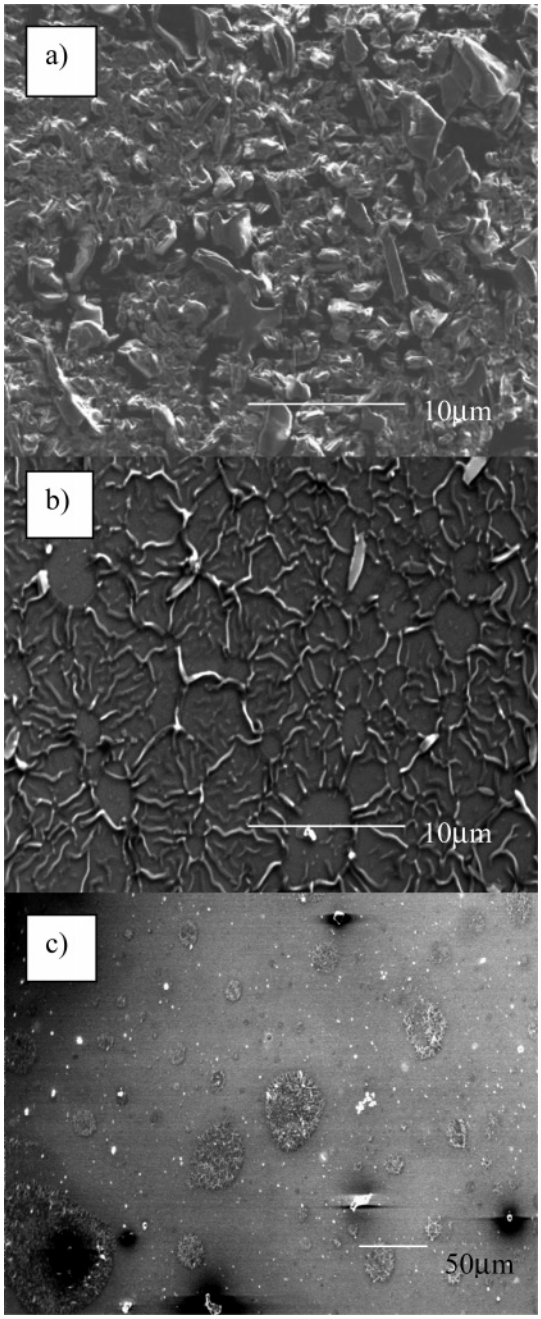

Figure 1. 10 μm scale scanning electron microscopy (SEM) images of films from (a) evaporated α-terthiophene (3T) and (b) polythiophene produced by 3T surface polymerization by ion-assisted deposition (SPIAD) for 1/150 $C_4H_4S^+$ ion/3T neutral ratio and 200 eV ion energy. (c) displays the same SPIAD polythiophene film as (b) on a larger scale.

graphitic carbon formed by direct thiophene ion deposition. Films deposited directly from mass-selected thiophene ions at the same ion energy and fluence as in Figure 1 are also featureless on the submicrometer scale (data not shown). Raman spectra indicated that these direct thiophene ion deposited films do not possess any oligo- or polythiophene structure and instead appear similar to sulfur-containing graphitic carbon.[18,19] The inelastically scattered background of the previously published XPS survey scans for the 3T SPIAD films shown in Figure 1c is performed using the QUASES software to elucidate further morphological information. It is estimated from the SEM image of Figure 1c that ∼30% of the film is composed of ∼50 μm diameter islands and the remaining ∼70% is the featureless region. The best QUASES fits are obtained by assuming that

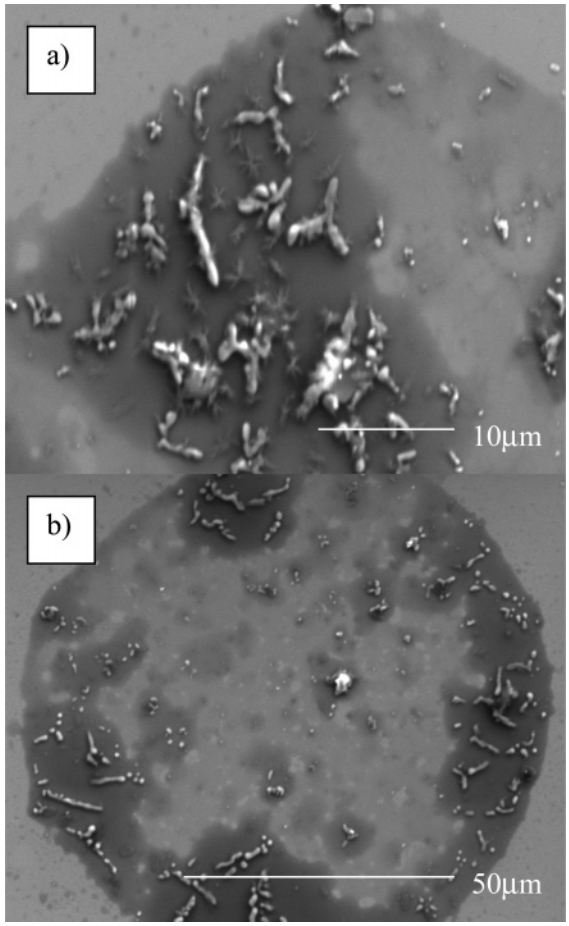

Figure 2. SEM of polythiophene film from 3T SPIAD at 1/450 ion/neutral ratio and 200 eV ion energy at two size scales: (a) 10 μm; (b) 50 μm.

the island layer thickness is 45−85 nm while the featureless layer is 7−20 nm thick. This fit is in agreement with the previous observation that SPIAD polythiophene films are much thicker than those from direct ion deposition at similar ion fluences and energies. By contrast, if the featureless region were bare silicon or a subnanometer thick organic layer, the average silicon content of the surface region would approach 70% rather than the ∼2% measured experimentally.[19] This further supports the argument that the featureless regions form by direct thiophene ion deposition. Previous estimates of the film thicknesses were ∼6 nm for the 3T SPIAD film and ∼3 nm for the direct ion deposited film, derived from calculation of the attenuation of the substrate Si_{2p} XPS peak assuming a uniform slab overlayer.[19] However, the discrepancy between the Si_{2p} attenuation and QUASES thicknesses is not surprising since both methods are semiquantitative. Also, the slab overlayer model is clearly not valid given the film morphology observed here.

Previous work on SPIAD showed the effect of ion/neutral ratio and ion energy on film chemical properties.[19] Morphology differences are also observed in SPIAD films due to variation in ion/neutral ratio for constant ion energy. Figure 2 shows SEM images of polythiophene films prepared at 1/450 ion/neutral ratio and 200 eV ion energy. The 1/450 ion/neutral ratio leads to the aggregation of grains into larger, longer, branched, and interconnected features shown in Figure 2a when compared with the 1/150 ion/neutral ratio films of Figure 1b,c. The 50 μm SEM image in Figure 2b shows that these elongated grain features are not evenly distributed over the larger film area, being most abundant at the island edges. The large circular islands observed

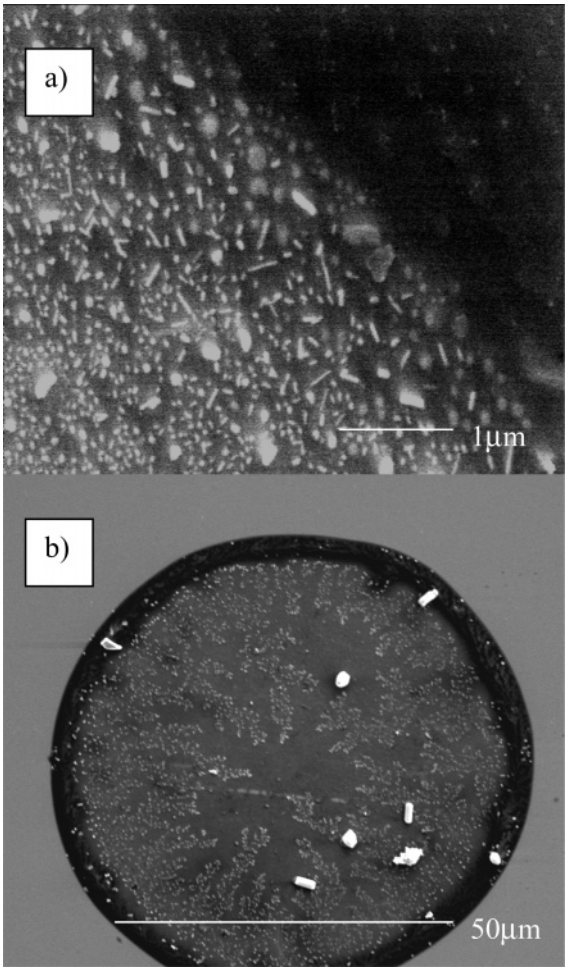

Figure 3. SEM of polythiophene film from 3T SPIAD at 1/150 ion/neutral ratio and 100 eV ion energy at two size scales: (a) 1 μm; (b) 50 μm.

in Figure 2b are of similar size distribution as those observed at 1/150 ion/neutral ratio and shown in Figure 1c.

Changes are also observed in morphology as the ion energy is varied for constant ion/neutral ratio. Figure 3 shows SEM images of polythiophene films prepared at 100 eV ion energy and 1/150 ion/neutral ratio. The 50 μm SEM image in Figure 3a shows the highest density of fractal-like features at the island edges, with the density decreasing toward the island center. The 1 μm image in Figure 3b recorded at the edge of the island shows small, elongated grains that are ~300 nm long and ~50 nm wide. Similar small elongated grains to those observed in Figure 3a for 100 eV SPIAD are not observed at the island edges in the 200 eV films shown in Figures 1 and 2. The 200 eV films in Figures 1 and 2 do not show any distinguished island edge region while, in Figure 3b, the island edge is prominent as a dark ring surrounding the island.

Attempts here to record XRD spectra of polythiophene films from mass-selected ion SPIAD have been unsuccessful, indicating either that the films are amorphous or their volume is insufficient to obtain diffraction patterns with the available instrumentation.

B. 3T SPIAD Films from Non-mass-Selected Ions. Polythiophene films produced by SPIAD with non-mass-selected thiophene ions and 3T neutrals show similar mass spectra and XPS to those observed with mass-selected SPIAD.[19] The appearance of mass spectral peaks attributed to 3T dimers (6T or other nonlinear structures) and 3T adducts with incorporated thiophene ion fragments confirms that ions play a critical role in film growth from non-mass-selected ions. Apparent similarities in the mechanism of surface polymerization observed for mass and non-mass-selected deposition[19,21] leads here to a comparison of their film morphology. Figure 4 shows SEM images of polythiophene films deposited from non-mass-selected ions at 1/100 ion/neutral ratio and 100 eV ion energy. Uniform features are observed over a 50 μm scale. Previously XRD experiments on polythiophene from non-mass-selected SPIAD showed crystalline structures where the most intense XRD peaks were attributed to 6T and 3T.[21]

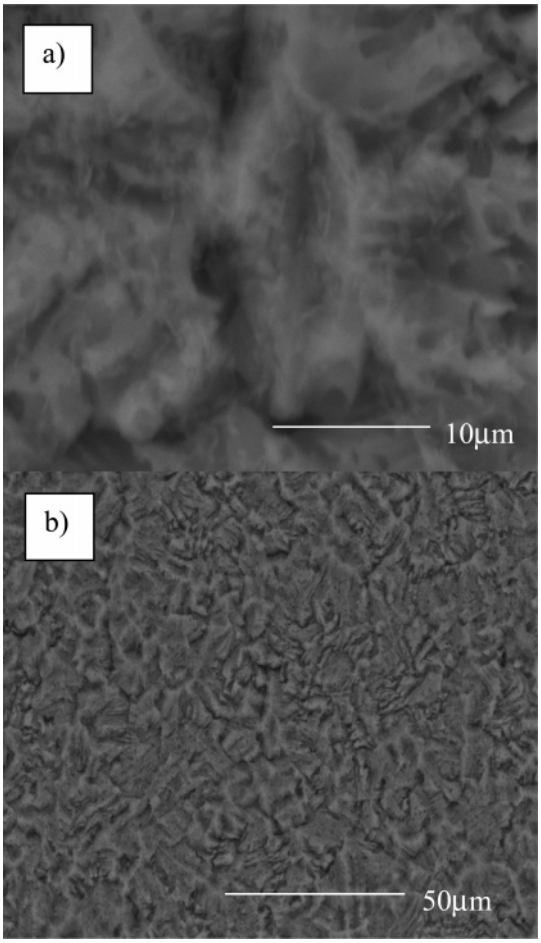

Figure 4. SEM of polythiophene films from non-mass-selected ion 3T SPIAD at (a) 10 μm and (b) 50 μm.

C. 3P SPIAD Films from Mass-Selected Ions. It was previously found that the use of a different neutral such as *p*-terphenyl (3P) creates a mixed SPIAD polyphenyl film with incorporated thiophene ions. Polyphenyl films prepared by SPIAD with 1/100 $C_4H_4S^+$ ion/3P neutral ratio and 200 eV ion energy grew faster and contained lower sulfur content than direct ion deposited films.[19] Mass spectra confirmed SPIAD polyphenyl films share many characteristics with SPIAD polythiophene films. SPIAD polyphenyl films consist of a mixture of species assigned to 3P multimers such as $[3P]_2^+$, adducts of 3P and thiophene ion such as $[3P]T^+$, and adducts of 3P with thiophene ion or 3P fragments such as $[3P]TC_xH_y^+$. Other data also supported the formation of a distribution of oligomers in the polyphenyl film with an extended electron conjugation length compared with evaporated 3P films.[19,23]

Figure 5 shows 10 μm scale SEM images of evaporated 3P and SPIAD polyphenyl films. The 3T evaporated film image in Figure 5a shows inhomogeneous needlelike islands of approximately constant width. These needles display elongated shapes, approximately 2 × 10 μm in size, which agglomerate

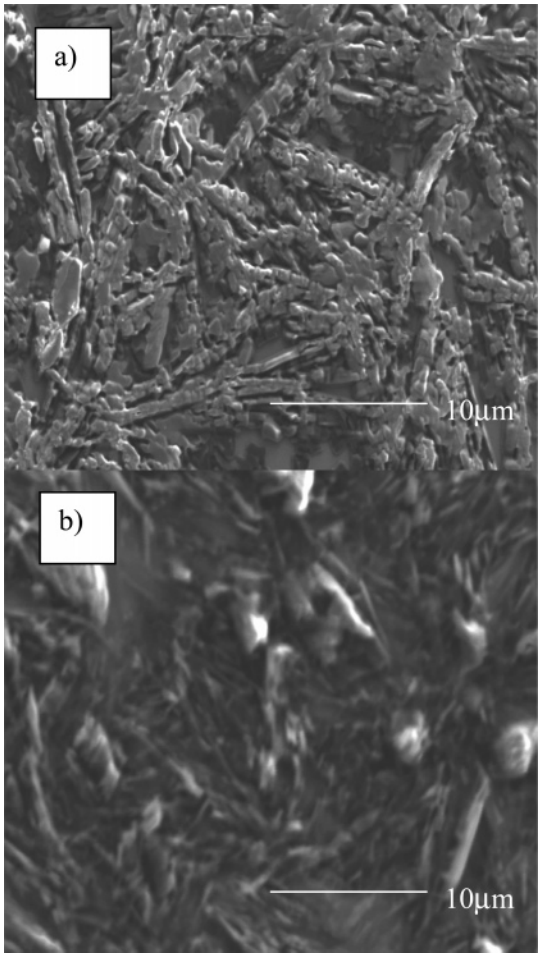

Figure 5. 10 μm scale SEM images of (a) evaporated *p*-terphenyl (3P) and (b) polyphenyl films from 3P SPIAD.

into ~10 μm wide starlike features similar to those observed previously.[27]

The 10 μm 3P SPIAD film image in Figure 5b displays both elongated and rounded grains. The elongated grains are similar to those seen in the 3P evaporated films of Figure 5a, while the rounded grains are ~2 μm across. However, the compact texture that results from the coexistence of these elongated and rounded grains differs from the starlike agglomerated features observed in the evaporated 3P film. Furthermore, SEM images of the 3P SPIAD films do not show formation of the islands observed in the 3T SPIAD film (i.e., Figure 1c). Rather, they do display a density distribution of the aforementioned features across the film corresponding to variations in ion fluence (not shown).

Figure 6 shows X-ray diffraction (XRD) of evaporated 3P and SPIAD polyphenyl films. 3P evaporated films show a crystalline XRD pattern, with all 3P peaks previously reported in the literature[27] and a Si substrate peak near 33°. The 3P SPIAD film also displays diffraction peaks characteristic of the 3P structure but does not show any new peaks. Two diffraction peaks at 19 and 21° that are present in the XRD of the evaporated 3P film disappear in the XRD of the polyphenyl film.

IV. Discussion

A. Morphology of Films from Mass-Selected Ions. SPIAD can control the overall polythiophene and polyphenyl film morphology through the mediation of adsorption, diffusion, sublimation (desorption), and other thermal film growth events by ion-induced processes including polymerization, sputtering, bond breakage, and energetic mixing.[13,19,22] The resultant film morphology manifests itself on various size scales, so the SEM data will be discussed below in order of decreasing feature size from the ~50 μm diameter islands observed for polythiophene films to the micrometer- and submicrometer-sized features that grow inside these islands.

3T SPIAD with mass-selected ions under the conditions reported here leads to the formation of a distribution of round and oval islands of polythiophene with diameters ranging from 10 to 100 μm sitting on a flat background of a sulfur-containing graphitic carbon (see Figures 1c and 2b). The average distance between thiophene ion impacts is <1 nm at these ion fluences, so it must be concluded that these ~50 μm diameter islands are not nucleated by single ion impacts. However, such polythiophene islands are not observed in the 3T evaporated films. It follows that these islands form as a result of the combined effects of neutral deposition, neutral sublimation, diffusion, and ion-induced processes. When molecules are physisorbed on a substrate surface, sublimation or desorption is expected to play an important role in the microscopic growth process.[28] One possible mechanism of island formation is that direct deposition of thiophene ions forms a sulfur-containing graphitic carbon layer onto which 3T is deposited. The continual deposition and sublimation of 3T leads to island formation which is then "frozen" in place by polymerization induced by the impact of additional thiophene ions. The similarity of the polythiophene island size and distribution at different ion/neutral ratios supports this argument, as ion fluence is varied while neutral fluence is kept constant. Within these islands, polymerization could nucleate the structures observed on the surface due to the formation of higher molecular weight, nonvolatile species. For example, 6T and other larger oligothiophenes desorb at higher temperatures and are therefore stable in a vacuum compared with 3T which readily undergoes sublimation.[1] The absence of these islands in the SPIAD polyphenyl films may relate to the lower rate of sublimation of 3P (which corresponds to the higher doser temperature required for 3P[19]). Furthermore, formation of these polythiophene islands films would probably be avoided by deposition onto cooled substrates which would minimize sublimation.

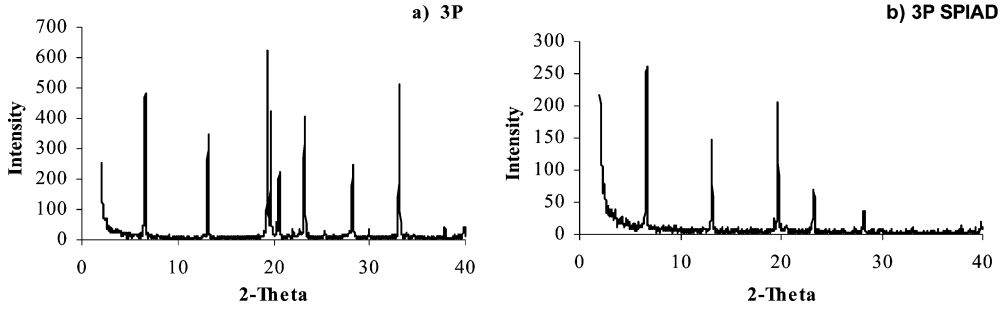

Figure 6. X-ray diffraction (XRD) of (a) evaporated 3P and (b) polyphenyl films from 3P SPIAD.

Ion-induced processes including polymerization, adduct formation, fragmentation, local heating, diffusion, and sputtering are affected by both ion/neutral ratio and ion energy. It was previously shown that polymerization in SPIAD varies from the most to least efficient for the conditions used in Figures 1−3, respectively.[19] Examination of the 10 μm image in Figure 1b of polythiophene shows that a lamellar network is formed on the surface by SPIAD. Similar lamellar networks were grown previously by controlling the substrate temperature of evaporated 6T films, where it was argued that the grain shape and orientation were governed by surface free energy.[6] The lamellar network of Figure 1b is replaced by fractal-like growth patterns in polythiophene for Figures 2 and 3. A general mechanism for fractal-like growth patterns was described by a cluster−cluster diffusion-limited aggregation process,[29] in which equal sized particles combine with each other to form dimers and then further aggregrate to form larger clusters in a fractal growth pattern. Formation of fractal-like structures in SPIAD could proceed by the adsorption of adjacent neutrals on the surface which are then polymerized by an ion impact to form higher molecular weight species which cannot readily undergo sublimation. Formation of these fractal-like aggregates is visible in the SEM image of the 100 eV polythiophene film in Figure 3b. Agglomeration of the 3T crystals begins along the island edges (dark ring in Figure 3b) where submicrometer, apparently crystalline grains form (see the 1 μm image shown in Figure 3a). Lower ion energy tends to form lower molecular mass weight species which will sublime more readily, contributing to the smaller size grains observed. These findings are in agreement with previous computational studies showing that increasing ion energy results in more damage to and sputtering of the film but also produces more polymerization initiators and therefore more efficient polymerization.[22]

Substrate templating often controls the morphology of thermally evaporated films.[1] However, the substrate generally has much less of an effect upon film morphology in hyperthermal ion-assisted processes[13] such as SPIAD, where the ion energy exceeds energetic barriers to surface diffusion by several orders of magnitude. The hyperthermal ion energies used here are sufficient to create surface defects, break neutral and ion bonds, and sputter surface species.[22] These and other ion-induced phenomena are expected to control SPIAD film morphology (beyond the large island formation events induced by evaporation). For this reason, this study has not examined the effect of substrate or film thickness upon morphology.

The crystallinity of these mass-selected ion deposited polythiophene films remains unknown since they are not observed here to diffract X-rays, but this absence of diffraction may be due to insufficient film volume. However, the images of polythiophene films in Figures 2a and 3a both display features that are strongly suggestive of crystallites. Furthermore, lamellar features similar those observed in Figure 1b for polythiophene are reminiscent of those previously observed for crystalline 6T films.[6] Previous results with NEXAFS showed these polythiophene films produced by SPIAD do not display a preferred orientation,[23] but a polycrystalline film is not necessarily inconsistent with the absence of diffraction. Lower substrate temperatures, ion energies, and ion/neutral ratios are expected to increase film crystallinity but will also reduce the extent of polymerization.

Comparing the morphology and XRD of the polyphenyl film from SPIAD on the same scale as the evaporated 3P film indicates a different balance between aggregation and other processes. Both elongated and rounded grains are present in the SPIAD polyphenyl film images in Figure 5b. XRD in Figure 6b indicates that the polyphenyl films preserve the crystallinity of the 3P evaporated film (Figure 6a). However, the disappearance of two important peaks may be due to changes in molecular orientation or packing upon polymerization.[30] Previous work showed the highest occupied molecular orbital of the polyphenyl film shifts down in binding energy[23] in a fashion similar to that observed when transitioning from coplanar to twisted *p*-polyphenyl films.[31] However, perhaps the most important factor in the polyphenyl film morphology is the reduced level of evaporation compared to the polythiophene films, which may explain the absence of fractal-like features in the polyphenyl films.

B. Morphology of Films from Non-mass-Selected Ions. Mass-selected ion SPIAD is currently practical only for small areas and very thin films, but non-mass-selected ion SPIAD produces thicker films over much larger areas from the broad beam Kaufman ion source. As a result, non-mass-selected ion SPIAD can be easily scaled up and prototyped for manufacturing purposes. Previous work found that the ∼150 nm thick polythiophene films produced by SPIAD non-mass-selected thiophene ions do display crystalline structure, with XRD peaks attributed to both 3T and 6T (and additional unidentified diffraction peaks).[21] These polythiophene films from non-mass-selected ion SPIAD show SEM images in Figure 6 that appear completely different than either evaporated 3T or any of the polythiophene images reported above. The Kaufman ion source produces radicals and photons which deposit on the surface along with the thiophene and fragment ions. The resultant radiative heating, photolysis, radicals and/or thiophene ion fragments apparently modify the micro- and nanostructures observed with mass-selected ion deposition.[20] The heating during deposition leads to rapid sublimation of excess 3T from the surface, as was observed directly with a quartz crystal microbalance.[21] The polythiophene film imaged in Figure 6 is also much thicker than those deposited by mass-selected ions (Figures 1−3). Different oligothiophenes are known to pack differently on a surface.[1,30] Collectively, these effects lead to a unique film structure, although it again appears that differences in sublimation−accelerated here by radiative heating−may be a dominant factor in determining film morphology.

V. Conclusions

A wide variety of structures form in the SPIAD polythiophene and polyphenyl films, including islands formed by sublimation, lamellar structures, nanoscale crystallites, and fractal-like growth patterns. The variation of these patterns with deposition conditions clearly indicate that ion-induced polymerization mediates film morphology through control of ion energy and ion/neutral ratio. Furthermore, these ion-assisted events mediate thermal processes such as neutral deposition and sublimation. Morphology can be controlled combinatorially by variation of substrate temperature, ion energy, ion or neutral structure, and ion/neutral ratio.[19] However, the above discussion does not consider all potentially significant phenomena, such as diffusion and dewetting. It is clear that a predictive understanding of how morphology develops in films during SPIAD is a complex interplay between thermal and ion-induced processes that will only avail itself through computer simulations of the controlling phenomenon.[28,32,33] Finally, the mass-selected SPIAD films are best suited for practical applications as they are thicker,[21] more uniform, more compact, display definite crystallinity, and produced by a method that is readily scalable to a manufacturing process.

Acknowledgment. This work is funded by the National Science Foundation (NSF) under Award No. CHE-0241425. We thank Professor Steve Guggenheim for use of his X-ray diffraction instrument and Alan Nichols for assistance with SEM in the Research Resources Center. Finally, L.H. would like to thank Bill Hase for his mentoring and past collaborations. His work is impeccable, his assistance unstinting, and his example to scientists everywhere without peer. Bill has been and continues to be everything a fine scientist should be.

References and Notes

(1) *Handbook of Oligo- and Polythiophenes*; Fichou, D., Ed.; Wiley-VCH: Weinheim, Germany, 1999.

(2) Adams, D. M.; Brus, L.; Chidsey, C. E. D.; Creager, S.; Creutz, C.; Kagan, C. R.; Kamat, P. V.; Lieberman, M.; Lindsay, S.; Marcus, R. A.; Metzger, R. M.; Michel-Beyerle, M. E.; Miller, J. R.; Newton, M. D.; Rolison, D. R.; Sankey, O.; Schanze, K. S.; Yardley, J.; Zhu, X.-Y. *J. Phys. Chem. B* **2003**, *107*, 6668.

(3) Schwartz, B. J. *Annu. Rev. Phys. Chem.* **2003**, *54*, 141.

(4) Hajlaoui, M. E.; Garnier, F.; Hassine, L.; Kouki, F.; Bouchriha, H. *Synth. Met.* **2002**, *129*, 215.

(5) Böhme, O.; Ziegler, C.; Göpel, W. *Synth. Met.* **1994**, *67*, 87.

(6) Servet, B.; Horowitz, G.; Ries, S.; Lagorsse, O.; Alnot, P.; Yassar, A.; Deloffre, F.; Srivastava, P.; Hajlaoui, R.; Lang, P.; Garnier, F. *Chem. Mater.* **1994**, *6*, 1809.

(7) Dillingham, T. R.; Cornelison, D. M.; Townsend, S. W. *J. Vac. Sci. Technol., A* **1996**, *14*, 1494.

(8) Soukopp, A.; Glöckler, K.; Schmitt, S.; Sokolowski, M.; Umbach, E.; Mena-Osteritz, E.; Bäuerle, P.; Hädicke, E. *Phys. Rev. B* **1998**, *58*, 13882.

(9) Iannotta, S.; Toccoli, T.; Biasioli, F.; Boschetti, A.; Ferrari, M. *Appl. Phys. Lett.* **2000**, *76*, 1845.

(10) Sassella, A.; Besana, D.; Borghesi, A.; Campione, M.; Tavazzi, S.; Lotz, B.; Thierry, A. *Synth. Met.* **2003**, *138*, 125.

(11) Podesta, A.; Toccoli, T.; Milani, P.; Boschetti, A.; Iannotta, S. *Surf. Sci.* **2000**, *464*, L673.

(12) Casalis, L.; Danisman, M. F.; Nickel, B.; Bracco, G.; Toccoli, T.; Iannotta, S.; Scoles, G. *Phys. Rev. Lett.* **2003**, *90*, 206101.

(13) Hanley, L.; Sinnott, S. B. *Surf. Sci.* **2002**, *500*, 500.

(14) Moliton, A. Ion implantation doping of electroactive polymers and device fabrication. In *Handbook of Conducting Polymers*, 2nd ed.; Skotheim, T. A., Elsenbaumer, R. L., Reynolds, J. R., Eds.; Marcel Dekker: New York, 1998; p 589.

(15) Usui, H. *Thin Solid Films* **2000**, *365*, 22.

(16) Fuoco, E. R.; Hanley, L. *J. Appl. Phys.* **2002**, *92*, 37.

(17) Hanley, L.; Choi, Y.; Fuoco, E. R.; Akin, F. A.; Wijesundara, M. B. J.; Li, M.; Tikhonov, A.; Schlossman, M. *Nucl. Instrum. Methods Phys. Res., Sect. B* **2003**, *203C*, 116.

(18) Tepavcevic, S.; Choi, Y.; Hanley, L. *J. Am. Chem. Soc.* **2003**, *125*, 2396.

(19) Tepavcevic, S.; Choi, Y.; Hanley, L. *Langmuir* **2004**, *20*, 8754.

(20) Choi, Y.; Tepavcevic, S.; Xu, Z.; Hanley, L. *Chem. Mater.* **2004**, *16*, 1924.

(21) Choi, Y.; Zachary, A.; Tepavcevic, S.; Wu, C.; Hanley, L. *Int. J. Mass Spectrom. Ion Processes* **2005**, *241*, 139.

(22) Hsu, W.-D.; Tepavcevic, S.; Hanley, L.; Sinnott, S. B. Submitted for publication, 2005.

(23) Tepavcevic, S.; Wroble, A. T.; Bissen, M.; Wallace, D. J.; Choi, Y.; Hanley, L. *J. Phys. Chem. B* **2005**, *109*, 7134.

(24) Wijesundara, M. B. J.; Ji, Y.; Ni, B.; Sinnott, S. B.; Hanley, L. *J. Appl. Phys.* **2000**, *88*, 5004.

(25) Tougaard, S. *J. Vac. Sci. Technol., A* **1996**, *14*, 1415.

(26) Tougaard, S. *Surf. Interface Anal.* **1998**, *26*, 249.

(27) Xie, R.; Fu, H.; Ji, X.; Yao, J. *J. Photochem. Photobiol., A* **2002**, *147*, 31.

(28) Campione, M.; Sassella, A.; Moret, M.; Marcon, V.; Raos, G. *J. Phys. Chem. B* **2005**, *109*, 7859.

(29) Jullien, R. *Comtemp. Phys.* **1987**, *28*, 477.

(30) Nagamatsu, S.; Kaneto, K.; Azumi, R.; Matsumoto, M.; Yoshida, Y.; Yase, K. *J. Phys. Chem. B* **2005**, *109*, 9374.

(31) Seki, K.; Karlsson, U.; Engelhard, R.; Koch, E.; Schmidt, W. *Chem. Phys.* **1984**, *91*, 459.

(32) Verlaak, S.; Steudel, S.; Heremans, P.; Janssen, D.; Deleuze, M. *Phys. Rev. B* **2003**, *68*, 195409.

(33) Boyd, K. J.; Marton, D.; Rabalais, J. W.; Uhlmann, S.; Frauenheim, T. *J. Vac. Sci. Technol., A* **1998**, *16*, 444.